BJ Biomolecules

Biochem. J. (2013) **452**, 57–66 (Printed in Great Britain) doi:10.1042/BJ20121832

Characterization of a pre-export enzyme–chaperone complex on the twin-arginine transport pathway

Jennifer M. DOW*, Frank GABEL†, Frank SARGENT*[1] and Tracy PALMER*[1]

*Division of Molecular Microbiology, College of Life Sciences, University of Dundee, Dundee DD1 5EH, U.K., and †Institut de Biologie Structurale, Commissariat à l'Energie Atomique, CNRS, Université Joseph Fourier, 41 rue Jules Horowitz, 38027 Grenoble, France

The Tat (twin-arginine translocation) system is a protein targeting pathway utilized by prokaryotes and chloroplasts. Tat substrates are produced with distinctive N-terminal signal peptides and are translocated as fully folded proteins. In *Escherichia coli*, Tat-dependent proteins often contain redox cofactors that must be loaded before translocation. Trimethylamine *N*-oxide reductase (TorA) is a model bacterial Tat substrate and is a molybdenum cofactor-dependent enzyme. Co-ordination of cofactor loading and translocation of TorA is directed by the TorD protein, which is a cytoplasmic chaperone known to interact physically with the TorA signal peptide. In the present study, a pre-export TorAD complex has been characterized using biochemical and biophysical techniques, including SAXS (small-angle X-ray scattering). A stable, cofactor-free TorAD complex was isolated, which revealed a 1:1 binding stoichiometry. Surprisingly, a TorAD complex with similar architecture can be isolated in the complete absence of the 39-residue TorA signal peptide. The present study demonstrates that two high-affinity binding sites for TorD are present on TorA, and that a single TorD protein binds both of those simultaneously. Further characterization suggested that the C-terminal 'Domain IV' of TorA remained solvent-exposed in the cofactor-free pre-export TorAD complex. It is possible that correct folding of Domain IV upon cofactor loading is the trigger for TorD release and subsequent export of TorA.

Key words: bacterial protein transport, *Escherichia coli*, molybdoenzyme, twin-arginine translocation protein transport pathway (Tat protein transport pathway), twin-arginine translocation proofreading chaperone (Tat proofreading chaperone).

INTRODUCTION

The Tat (twin-arginine translocation) protein transport pathway exports proteins across the cytoplasmic membranes of bacteria and archaea, and the thylakoid membranes of plant chloroplasts [1,2]. Protein substrates of the Tat pathway are folded before translocation and are targeted to the Tat machinery by cleavable N-terminal signal peptides containing an almost invariant pair of arginine residues [3]. Transport by the Tat pathway is energized solely by the protonmotive force [1,2].

The model bacterium *Escherichia coli* K-12 produces 28 proteins bearing twin-arginine signal peptides. Approximately two-thirds of these proteins are known or predicted to contain redox cofactors and some of them also form complexes with partner subunits that lack a signal peptide before export [4]. The complexity of these Tat substrates necessitates a pre-export 'proofreading' process to ensure that only folded and assembled proteins are presented for translocation. One hypothesis involves dedicated chaperone proteins that interact directly with twin-arginine signal peptides to prevent premature targeting of the substrate before cofactor insertion and binding of any protein partners [5].

The *E. coli* TMAO (trimethylamine *N*-oxide) reductase TorA is a soluble periplasmic enzyme containing the MGD (molybdopterin guanine dinucleotide) cofactor at its active site [6]. TorA is a well-characterized substrate of the Tat pathway; indeed, transport of TorA to the periplasm was found to be blocked in a mutant strain that was unable to synthesize MGD, which led to the original hypothesis that a transport pathway for folded proteins may exist in bacteria [7]. The TorA protein is encoded by the *torCAD* operon (Figure 1A) where TorC is a haem-containing quinol oxidase and TorD is a cytoplasmic protein [8]. Cellular levels of enzymatically active TorA are significantly reduced in a strain lacking the *torD* gene [9], and the TorD protein was found subsequently to interact with an unfolded (heat-denatured) form of the mature TorA enzyme [9]. This initial work therefore established that there was a clear binding site for TorD within the mature region of the protein and suggested a role for TorD in loading the MGD cofactor into the TorA apoenzyme [9,10]. In addition to this, a subsequent genetic screen identified TorD as a binding partner for the TorA twin-arginine signal peptide [11]. This was confirmed *in vitro* when recombinant TorD was shown to bind directly to the isolated TorA signal peptide with a 1:1 stoichiometry and an apparent K_d of ~59 nM [12,13]. The binding epitope for TorD has been mapped to the C-terminal end of the TorA signal peptide, close to its junction with the mature portion of the enzyme [12,14]. Interestingly, binding of the TorA signal peptide by TorD seems to be an activity not strictly connected with cofactor loading, since co-expression of *torD* can enhance the export of synthetic signal peptide fusion proteins on the Tat pathway [11,15]. The TorD protein itself is 22.5 kDa and is known to exist in equilibrium between monomeric and dimeric forms [16–18], have a low level of GTPase activity associated with the dimeric form [18], and have the ability to bind the MGD cofactor *in vitro* [19]. However, although it is clear that the monomeric form of TorD can bind the isolated TorA signal peptide [12,13], the physiological role and significance of TorD dimerization is not clear.

Current models for TorA biosynthesis assume that TorD interacts with the TorA precursor by binding at two distinct sites: one being within the twin-arginine signal peptide with the other, uncharacterized, site lying elsewhere in the mature portion

Abbreviations used: DTT, dithiothreitol; ICP-MS, inductively coupled plasma–MS; IMAC, immobilized metal-ion-affinity chromatography; LB, Luria–Bertani; MALLS, multi-angle laser light scattering; MGD, molybdopterin guanine dinucleotide; SAXS, small-angle X-ray scattering; SEC, size-exclusion chromatography; SPA, sequential peptide affinity; Tat, twin-arginine translocation; TMAO, trimethylamine *N*-oxide.

[1] Correspondence may be addressed to either of these authors (email f.sargent@dundee.ac.uk or t.palmer@dundee.ac.uk).

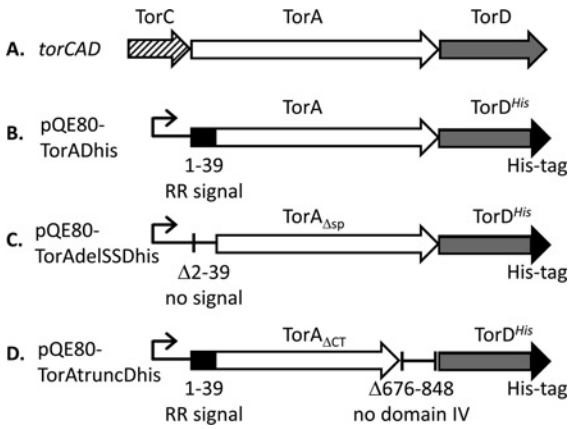

Figure 1 Tools for the isolation of TorAD complexes

(**A**) A cartoon representing the structure of the *torCAD* operon located at 22.8 min on the *E. coli* chromosome. The names of the protein products of the genes are given above the arrows. (**B**) An overexpression vector based on pQE80 (Qiagen) encoding full-length TorA and TorD^{His}. The natural transcriptional and translational coupling between *torA* and *torD* is maintained. (**C**) An expression vector encoding TorA lacking its entire Tat signal peptide comprising Asn^{2}–Ala^{39} (TorA$_{\Delta sp}$, TorA Δ2–39) and TorD^{His}. (**D**) An expression vector encoding TorA lacking its entire C-terminal Domain IV comprising Ile^{676}–Ser^{848} (TorA$_{\Delta CT}$, TorA Δ676–848) and TorD^{His}.

of the protein [5,20]. These two binding events are thought to not only delay the Tat transport event, but also actively facilitate efficient insertion of the MGD cofactor into the apoenzyme. This pre-export 'Tat proofreading' process would be completed by the controlled release of the bound chaperones and subsequent translocation of the folded active enzyme to the periplasm. However, it is not known whether each of the TorD-binding sites on the TorA apoenzyme are bound by separate TorD monomers or a single TorD dimer, or whether the TorD monomer itself contains two distinct TorA-binding sites. Moreover, the degree of folding of the TorA precursor when bound by TorD has not been explored, and it remains a mystery how release of the chaperones is ultimately triggered.

In the present study, a stable and cofactor-free complex of TorD with the TorA apoenzyme has been isolated, both with and without the twin-arginine signal peptide. Using a combination of biophysical and biochemical approaches, we have demonstrated that a single TorD monomer binds directly to a single TorA apoprotein regardless of the presence of the signal peptide. This suggests that a single TorD monomer recognizes two binding sites on the TorA polypeptide and that these epitopes are nearby or overlapping. Finally, we have demonstrated that binding of TorA by TorD changes the conformation of apo-TorA in relation to the mature active enzyme by inducing exposure of the C-terminal domain of the TorA protein.

EXPERIMENTAL

Plasmid and strain construction

The *torAD* genes form a transcription unit on the *E. coli* chromosome with overlapping stop and start codons. To co-overproduce TorA and TorD^{His}, this natural translational coupling was retained. DNA encoding SPA (sequential peptide affinity)-tagged TorD along with TorA was amplified from the chromosome of *E. coli* strain DY330 *torD-SPA* [21,22] using oligonucleotides TorAMfeIup (5′-GCGCCAATTGCGATAAGAAGGAAGAAA-AATAATG-3′) and SPASphIdown (5′-GCGCGCATGCCTACT-TGTCATCGTCATCC-3′). The resulting PCR product was digested with MfeI and SphI and cloned into pQE80 digested previously with EcoRI and SphI. To replace DNA encoding the SPA-tagged variant of TorD with a His-tagged variant, the pQE80torADSPA plasmid was digested with NheI (which removes DNA covering the 3′-end of *torD*, the SPA-tag-coding sequence and a small region of the vector). Plasmid pQE60torD [13] which codes for a C-terminally His-tagged TorD was also digested with NheI and the fragment covering the 3′-end of *torD* along with the His-tag-coding sequence was ligated into the digested pQE80torADSPA vector. Resultant clones were analysed by sequencing to ensure that the NheI fragment had been cloned into the correct orientation, and the construct was designated pQE80TorADhis (Figure 1B).

To overproduce TorD^{His} along with TorA lacking its N-terminal signal peptide, the encoding DNA was amplified using oligonucleotides TorAMfeIdelSS (5′-GCGCCAATTGCGATAA-GAAGGAAGAAAAATAATGGCGCAAGCGGCGACTGACG-CTGTCATCTCG-3′) and QEreverse (5′-GTTCTGAGGTCATT-ACTGGAT-3′), with pQE80 TorADhis as a template. The resultant PCR product was digested with MfeI and HindIII and cloned into pQE80 that had been pre-digested with EcoRI and HindIII, to give construct pQE80TorAdelSSDhis (Figure 1C).

To produce a C-terminally truncated TorA along with TorD^{His}, a fragment of *torA* terminating at codon 675 and followed by a stop codon was amplified with oligonucleotides TorAfor (5′-GACCTCAACCTGCCGCTTTGC-3′) and TorA675STOP HindIII (5′-GCGCAAGCTTATTTCTCAAACCACATCGGAT-GCCC-3′) and digested with NruI (the recognition site for which is present in the *torA* gene) and HindIII. A second PCR product covering the *torD* ribosome-binding site and a fragment of the *torD* gene was amplified with oligonucleotides TorDHindRBS (5′-GCGCAAGCTTGCAGGTGAAATCATGACCACG-3′) and TorDrev (5′-GGTCATCAGAAACAGGCCGC-3′) and digested with HindIII and SacII (the recognition site for SacII occurs naturally in *torD*). A three-way ligation was carried out with these two fragments and pQE80TorADhis that had been digested previously with NruI and SacII. The resultant clone was designated pQE80TorAtruncDhis (Figure 1D).

Strain FTH007 encodes a C-terminally hexahistidine-tagged TorA produced from the native chromosomal location and was constructed as follows. A 582 bp fragment of *torA* DNA finishing immediately before the *torA* stop codon was amplified with oligonucleotides TorAHis1 (5′-GCGCCCATGGCTCGAAAAC-TATCGCCGATATGAAC-3′) and TorAHis2 (5′-GCGCAGAT-CTTGATTTCACCTGCGACGCGGGAAC-3′), digested with NcoI and BglII and cloned into similarly digested pFAT210 [23]. DNA covering the *torD* ribosome-binding site and approximately 600 nucleotides of downstream DNA was amplified with oligonucleotides TorAHis3 (5′-GCGCAAGCTTTGTTCCCGC-GTCGCAGGTGAAATC-3′) and TorAHis4 (5′-GCGCTCTAG-AGACGTTATCTGTTTTGGTGGTCGC-3′), digested with XbaI and HindIII and cloned into the above construct. DNA covering the *torAhis* allele was subsequently excised by digestion with XbaI and KpnI and cloned into similarly digested pMAK705 [24]. The *torAhis* allele was then moved on to the chromosome of strain DSS401 (as MC4100, Δ*dmsABC*::Kan^{R}) [25] to give strain FTH007.

All constructs were fully sequenced to ensure that no mistakes had been introduced inadvertently during the cloning procedure.

TMAO reductase assays

TMAO reductase assays were performed using strain GB426 (as MC4100, Δ*torCAD*::Apr^{R}, Δ*dmsABC*::Kan^{R} [22]), which contained either pQE80, pQE80TorADhis, pQE80TorAdelSSDhis

or pQE80TorAtruncDhis. Cells were cultured anaerobically overnight in LB (Luria–Bertani) medium supplemented with 0.5 % glycerol and 0.4 % TMAO, along with the antibiotics apramycin (50 μg/ml), kanamycin (25 μg/ml) and ampicillin (100 μg/ml). Cells were harvested, washed and lysed by passage through a French press pressure cell as described previously [26]. After removal of unbroken cells and debris by a short centrifugation step, the resultant crude cell extract was assayed for TMAO reductase activity essentially as described previously [6,27]. Protein concentration was determined using the Lowry assay [28].

Preparation of recombinant proteins

All plasmid-encoded TorA/TorD^{His} proteins were overproduced and purified in an identical manner. A single colony of freshly transformed *E. coli* BL21(DE3) [F^- *ompT hsdS*(r_B^- m_B^-) *gal dcm* λ(DE3)] was cultured overnight in 5 ml of LB medium supplemented with 100 μg/ml ampicillin. This provided the inoculum for a 500 ml culture, which was grown aerobically at 37 °C and at 140 rev./min in a baffled 2 litre flask to a D_{600} of 0.6 before induction of recombinant protein production by addition of 2 mM IPTG (isopropyl β-D-thiogalactopyranoside), followed by a temperature shift to 18 °C. After 16 h, cells were harvested and resuspended (10 ml per 1 g of cells) in buffer A [50 mM Tris/HCl (pH 7.5), 200 mM KCl, 1 mM DTT (dithiothreitol) and 25 mM imidazole]. Protease inhibitor [EDTA-free Complete™ protease inhibitor cocktail (Roche)], lysozyme and DNase were added to the resuspension and cells were lysed using an Emulsiflex C3 high-pressure homogenizer. Cell debris was removed by centrifugation at 18 850 ***g*** for 15 min, followed by removal of membranes by ultracentifugation at 45 000 rev./min for 1 h using a Beckman Ti70 rotor. All centrifugation steps were conducted at 4 °C. The supernatant obtained following ultracentrifugation was filtered through a 0.22-μm-pore-size membrane filter (Millipore) before being subjected to IMAC (immobilized metal-ion-affinity chromatography) as follows. The extract was loaded on to a 5 ml HisTrap column (GE Healthcare) equilibrated with buffer A. After extensive washing with buffer A, hexahistidine-tagged proteins were subsequently eluted using a gradient of 25–500 mM imidazole in buffer A. TorA/TorD^{His}-containing fractions were identified by SDS/PAGE (12% gels), pooled and concentrated to 2 ml using a Vivaspin 20 spin concentrator (10 kDa cut-off, Sartorius). The concentrated sample was then loaded on to a calibrated HiLoad 16/60 Superdex 200 Prep Grade (GE Healthcare) size-exclusion column equilibrated with buffer A (50 mM Tris/HCl, pH 7.5, 200 mM KCl and 1 mM DTT), with TorA/TorD^{His}-containing fractions again identified by SDS/PAGE (12% gels).

Chromosomally encoded TorA^{His} was purified from cells that had been cultured anaerobically in 5 litre capped bottles that had been filled with LB medium supplemented with 0.4 % TMAO, 0.5 % glycerol and 50 μg/ml kanamycin. After inoculation with a 5 ml pre-culture, bottles were incubated for 16 h without shaking at 37 °C. Cells were harvested, washed and resuspended to a final concentration of 10 ml/g of cells in 50 mM Tris/HCl (pH 7.5) and 40 % (w/v) sucrose. The suspension was then supplemented with EDTA (5 mM final concentration) and 0.6 mg/ml lysozyme and incubated for 30 min at 37 °C to release the periplasmic fraction. Sphaeroplasts were removed by centrifugation at 12 500 rev./min for 20 min using a Beckman JA-25.50 rotor at 4 °C and the supernatant was retained. The EDTA was removed by dialysis in buffer A before loading the supernatant on to a 5 ml HisTrap column and purifying as above.

SAXS (small-angle X-ray scattering)

SAXS data using purified TorD^{His}, TorA/TorD^{His} and TorA$_{\Delta SP}$/TorD^{His} samples were recorded on the ID14-3 BioSAXS beamline at the European Synchrotron Radiation Facility (ESRF Grenoble, France). Sample-detector distance was 2.43 m for an X-ray wavelength of 0.931 Å (1 Å = 0.1 nm). Then, 50 μl sample and buffer volumes were loaded in a flowthrough quartz capillary cell at 25 °C. The sample volume exposed to the X-ray beam was approximately 10 μl. Samples were checked for radiation damage by using ten successive exposure times of 10 s each. Final exposure time was 100 s for all samples/buffers. The two-dimensional diffraction patterns were normalized to an absolute scale and azimuthally averaged to obtain the intensity profiles I(Q), within BSxCuBE (ESRF beamline data collection software). Solvent contributions (buffer backgrounds collected before and after every protein sample) were averaged and subtracted from the associated protein sample using the program PRIMUS [29].

CD analysis

CD analysis of protein samples was provided as a service by the Scottish Circular Dichroism Facility, University of Glasgow. Spectra of protein solutions were obtained using a JASCO J-810 spectropolarimeter. Far-UV CD measurements (185–260 nm) were collected in quartz cells of 0.02 cm pathlength at 25 °C with a scan speed of 10 nm/min, bandwidth of 1 nm, response of 2 s and data pitch of 0.2 nm. Before collection of CD data, proteins were buffer-exchanged into CD-appropriate buffer (50 mM Tris/H_2SO_4, pH 7.5, 200 mM K_2SO_4 and 1 mM DTT). Protein concentrations were estimated using a NanoDrop spectrophotometer before the experiment. Near-UV CD measurements (250–320 nm) were obtained in a 0.2-cm-pathlength quartz cuvette using the following parameters: temperature, 25 °C; scan speed, 10 nm/min; bandwidth, 1 nm; response, 2.0 s; and data pitch, 0.2 nm. Protein was analysed in appropriate buffer (50 mM Tris/HCl, pH 7.5, 200 mM KCl and 1 mM DTT). The spectra were corrected for protein concentration and cell pathlength before being analysed by DichroWeb (http://dichroweb.cryst.bbk.ac.uk), an online server which hosts the various algorithms used to estimate protein secondary structures.

Metal analysis

Metal content was analysed by ICP-AES (inductively coupled plasma–atomic emission spectrometry)/ICP-MS (inductively coupled plasma–MS) and was provided as a service by the School of Chemistry at the University of Edinburgh.

Limited trypsinolysis of TorA–TorD^{His} and TorA$_{\Delta SP}$–TorD^{His} complexes

Protein samples (1 mg/ml in 50 mM Tris/HCl, pH 7.5, 200 mM KCl and 1 mM DTT; 100 μl final volume) were incubated with 1 % (w/w) trypsin (porcine pancreas, proteomics grade, Sigma–Aldrich) at 37 °C. Aliquots of 5 μl were withdrawn at various intervals and the reaction stopped by addition of 20 μl of Laemmli buffer (Bio-Rad Laboratories) followed by immediate boiling for 10 min. Once the time course was completed, samples were analysed by SDS/PAGE (12% gels).

Proteins were identified by tryptic peptide mass fingerprinting of gel slices performed by the FingerPrints Proteomic Service (College of Life Sciences, University of Dundee).

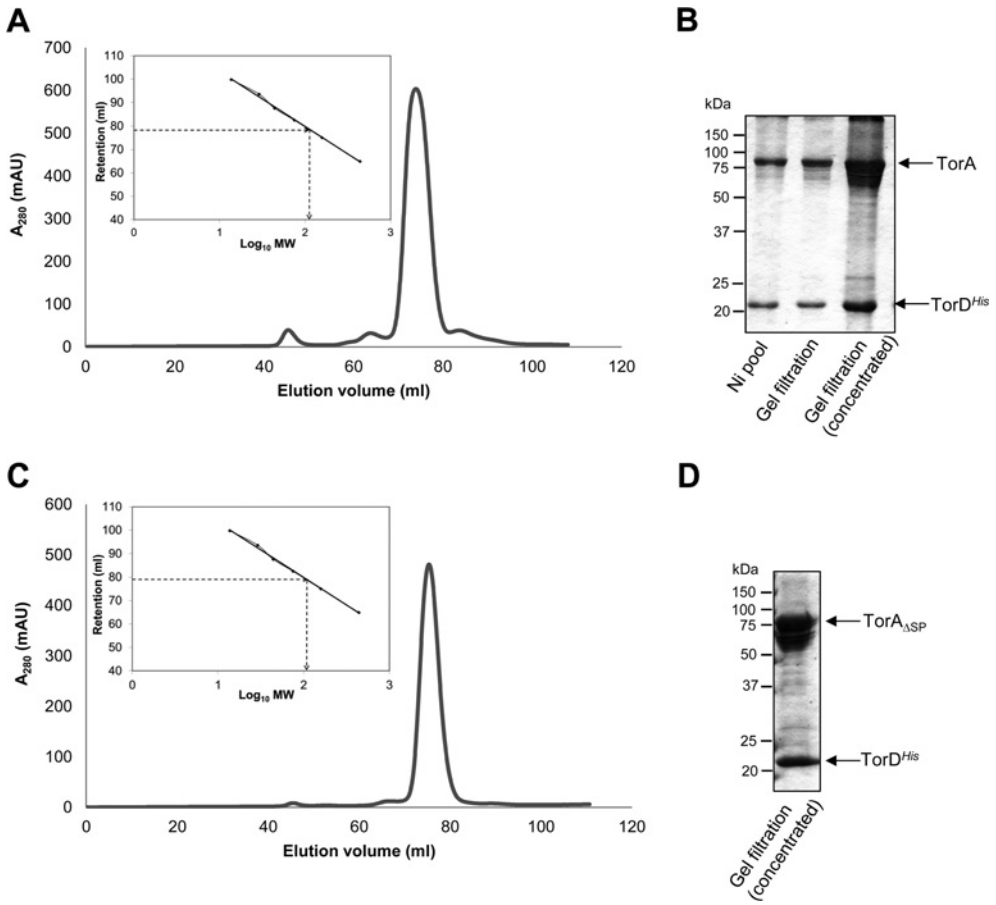

Figure 2 Isolation of a TorA–TorD^{His} and TorA$_{\Delta SP}$–TorD^{His} complex

(**A** and **C**) TorD^{His}-containing fractions after metal chelate chromatography of cell extracts overproducing (**A**) TorA and TorD^{His} or (**C**) TorA$_{\Delta SP}$ and TorD^{His} were pooled, concentrated and applied to a HiLoad 16/60 Superdex 200 Prep Grade size-exclusion column. Eluted protein was monitored by measuring absorbance at 280 nm. The column was calibrated with the standard proteins ribonuclease (14 kDa), carbonic anhydrase (29 kDa), ovalbumin (44 kDa), conalbumin (75 kDa), aldolase (158 kDa) and ferritin (440 kDa), and the linear regression analysis is shown as inset boxes. $R^2 = 0.9976$, $y = -23.5x + 126.83$. MW, molecular mass. (**B** and **D**) SDS/PAGE analysis (12 % gels) of (**B**) the concentrated fractions after metal chelate chromatography (Ni pool), and the non-concentrated and concentrated peak fractions from SEC of the TorA–TorD^{His} complex and (**D**) the concentrated peak fraction from SEC of the TorA$_{\Delta SP}$–TorD^{His} complex. Molecular masses are indicated in kDa.

Analysis of TorA–TorD^{His} complexes by SEC (size-exclusion chromatography)–MALLS (multi-angle laser light scattering)

Size estimates of TorA–TorD^{His} complexes were obtained by SEC–MALLS, which was provided as a service by the University of York Bioscience Technology Facility. Measurements were conducted on a system comprising a Wyatt HELEOS-II multi-angle light-scattering detector and a Wyatt rEX refractive index detector linked to a Shimadzu HPLC system (SPD-20A UV detector, LC20-AD isocratic pump system, DGU-20A3 degasser and SIL-20A autosampler). Work was conducted at room temperature (20 ± 2 °C). Solvent was filtered through a 0.2-μm-pore-size filter before use and a further 0.1-μm-pore-size filter was present in the flow path. Filtered (0.2 μm pore size) TorA–TorD^{His} samples (100 μl, corresponding to 100 μg of protein) were applied to a Superdex 200 10/300 GL column (GE Healthcare) equilibrated with 50 mM Tris/HCl (pH 7.5), 200 mM KCl and 1 mM DTT at 0.5 ml/min; Shimadzu LC Solutions software was used to control the HPLC, and Astra V software was used for the HELEOS-II and rEX detectors. BSA was used for molecular mass calibration. The Astra data collection was 1 min shorter than the LC solutions run to maintain synchronization. Blank buffer injections were used as appropriate to check for carry-over between sample runs. Data were analysed using the Astra V software. MWs were estimated using the Zimm fit method [30] with degree 1. A value of 0.19 was used for protein refractive index increment (dn/dc).

RESULTS

Isolation of a TorA–TorD^{His} complex

Isolation of a complex between untagged TorA and affinity-tagged TorD was originally demonstrated on a small scale using a C-terminally SPA-tagged form of TorD [22]. In order to scale up the co-expression system to allow detailed analysis of the complex, the original *torAD^{SPA}* allele was cloned into expression vector pQE80 and the DNA coding for the SPA tag at the C-terminus of TorD replaced with a hexahistidine tag (Figure 1B). The soluble cell extract containing overproduced TorA and TorD^{His} was subjected to IMAC and fractions containing proteins of the expected size of TorA and TorD^{His} were identified in a single peak at 110 mM imidazole. The IMAC samples were pooled, concentrated and subjected to SEC using a HiLoad 16/60 Superdex 200 Prep Grade column. As shown in Figure 2(A), protein was eluted at 78.5 ml, corresponding to an estimated molecular mass of 114 kDa. Analysis of the peak fraction

by SDS/PAGE revealed the presence of two major proteins (Figure 2B), which were confirmed by tryptic peptide mass fingerprinting to be TorA and TorD^{His}. The overall protein yield from this process was approximately 1.5 mg/g of bacterial cells.

It was notable during the purification of TorAD^{His}, particularly following concentration of the samples, that more than one electrophoretic form of TorA was evident by SDS/PAGE. A low-percentage acrylamide gel was therefore used to separate these forms, which were excised and analysed by tryptic peptide mass fingerprinting. The analysis showed that, whereas the majority of the TorA was present as full-length intact polypeptide, there was a proportion of TorA that had undergone limited proteolysis and was lacking up to 150 amino acids from its C-terminal end (Supplementary Figure S1 at http://www.biochemj.org/bj/452/bj4520057add.htm). In addition, in some instances, up to 12 amino acid residues could be lost from the N-terminus of TorA. It is concluded that, whereas a complex of TorAD^{His} is stable to purification, the extremities of TorA can be subjected to variable levels of proteolysis during isolation.

Removal of the entire Tat signal peptide from the TorA protein (TorA Δ2–39) still allows isolation of a stable complex with TorD^{His}

As well as signal peptide binding, previous biochemical and genetic experiments pointed to a binding site for TorD within the mature region of the TorA enzyme (e.g. [9,10]). To investigate this further, a vector was designed that would co-overproduce a version of TorA lacking its entire 39-residue Tat signal peptide (TorA$_{\Delta SP}$) with TorD^{His} (Figure 1C). When TorD^{His} was isolated from the soluble cell fraction by IMAC, a protein of the expected size of TorA$_{\Delta SP}$ was also co-purified. The TorD^{His}-containing fractions were pooled, concentrated and applied to a Superdex 200 size-exclusion column. The TorD^{His} eluted at 78.8 ml, corresponding to an estimated molecular mass of 110 kDa (Figure 2C) and analysis of the concentrated peak fraction by SDS/PAGE revealed the presence of two major proteins (Figure 2D), which were confirmed by tryptic peptide mass fingerprinting to be TorA$_{\Delta SP}$ and TorD^{His}. Thus it is clear that a stable complex of TorD^{His} and TorA can be isolated in the absence of the twin-arginine signal peptide.

TorD^{His} binds the full-length TorA precursor, and the TorA$_{\Delta sp}$ species lacking its entire signal peptide (Δ2–39), at a 1:1 stoichiometry

SEC indicates that the complex of TorD^{His} with TorA elutes at a similar molecular mass regardless of whether the signal peptide was present on TorA (Figure 2). A more accurate technique is SEC–MALLS, which uses HPLC-linked SEC coupled with static laser light scattering to provide a direct measure of molecular mass. Using this technique, the TorA–TorD^{His} complex was observed to exhibit a mass range of 100–120 kDa and a peak mass of 114.7 kDa (Table 1), which is very close to the calculated mass (117.9 kDa) for a 1:1 complex of the two proteins (Table 1). The TorA$_{\Delta SP}$–TorD^{His} complex exhibited a mass range of 95–115 kDa and a peak mass of 108.2 kDa (Table 1), which is close to the calculated theoretical mass (113.8 kDa) for a 1:1 complex of the two proteins (Table 1). The relatively wide mass range seen for both samples reflects the observed proteolytic events leading to heterogeneity of the TorA sample observed by SDS/PAGE (Figure 2). Overall, the SEC–MALLS analyses point to complexes containing one TorA protein and one TorD protein, and suggest strongly that TorD can remain stably bound to TorA in the absence of the twin-arginine signal peptide.

Table 1 The apparent molecular masses of TorAD complexes

Parameters obtained from SEC–MALLS analysis of each of the indicated complexes.

Sample	Major peak elution range (min)	Molecular mass at peak (kDa)	Range across peak (kDa)	Predicted molecular mass of a 1:1 complex (kDa)
TorA–TorD^{His}	26.4–30.4	114.7	100–120	117.9
TorA$_{\Delta SP}$–TorD^{His}	26.3–30.0	108.2	95–115	113.8
TorA$_{\Delta CT}$–TorD^{His}	27.6–30.2	99.7	97–107	99.2

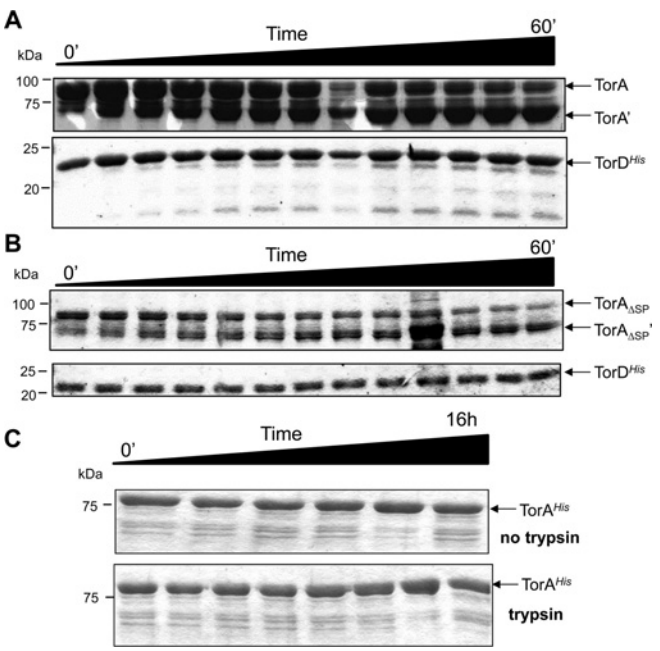

Figure 3 Limited trypsinolysis of the TorA–TorD^{His} and TorA$_{\Delta SP}$–TorD^{His} complexes

The TorA–TorD^{His} (**A**) and TorA$_{\Delta SP}$–TorD^{His} complexes (**B**) were isolated. Each purified complex was incubated with trypsin and 5 μl aliquots removed at 5 min intervals between 0 and 60 min, mixed with Laemmli buffer and immediately boiled to prevent any further digestion. (**C**) As a control, periplasmic mature TorA^{His} was purified and incubated with trypsin before 5 μl aliquots were removed at the following eight time points (0 min, 10 min, 20 min, 30 min, 1 h, 2 h, 4 h and 16 h). Concomitantly, mature TorA^{His} incubated without trypsin before aliquots were removed at the following six time points (0 min, 10 min, 30 min, 1 h, 4 h and 16 h). Samples were mixed with Laemmli buffer and immediately boiled. At the end of the time courses, the samples were analysed by SDS/PAGE (12 % gels). Molecular masses are indicated in kDa.

The TorA C-terminal domain is protease-accessible in TorAD complexes

To gain more insight into the architecture of the TorAD complexes under investigation in the present study, limited proteolysis experiments were undertaken. First, the purified TorA–TorD^{His} complex was incubated with a low concentration of trypsin over a time course of 60 min. As shown in Figure 3(A), TorD^{His} was almost completely resistant to trypsinolysis under these conditions. In contrast, TorA was cleaved to yield a stable proteolytic fragment of approximately 70 kDa that was apparently resistant to further digestion by trypsin. Peptide mass fingerprinting of the stable 70 kDa TorA proteolysis product revealed that the initial 675 amino acid residues from the N-terminus of the protein were intact and that the trypsin treatment had therefore removed a short section of polypeptide from the C-terminal end of TorA (Supplementary Figure S1).

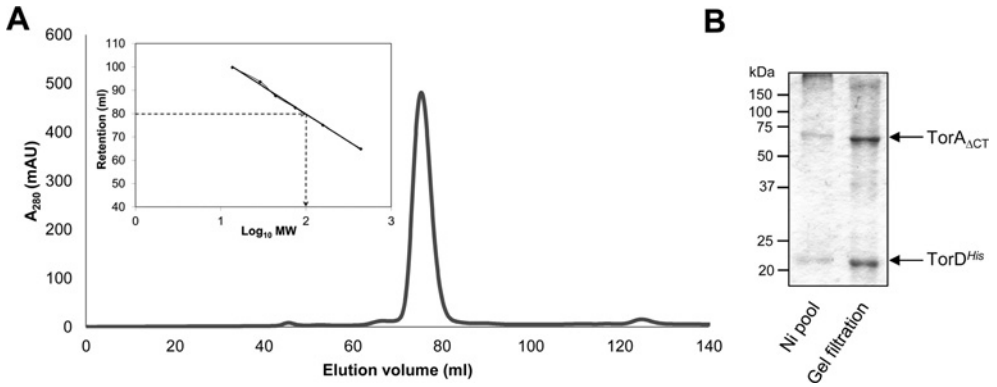

Figure 4 Domain IV of TorA is not required for complex formation with TorD

(**A**) $TorD^{His}$-containing fractions after metal chelate chromatography of cell extracts overproducing $TorA_{\Delta CT}$ and $TorD^{His}$ were pooled, concentrated and applied to a HiLoad 16/60 Superdex 200 Prep Grade size-exclusion column. Eluted protein was monitored by measuring absorbance at 280 nm. MW, molecular mass. (**B**) SDS/PAGE analysis (12 % gels) of the pooled fractions after metal chelate chromatography (Ni pool), and the non-concentrated peak fraction following gel-filtration chromatography. Molecular masses are indicated in kDa.

Next, the $TorA_{\Delta SP}$–$TorD^{His}$ complex, where TorA had already had its 39-residue signal peptide deliberately removed, was incubated with trypsin in a similar manner. As shown in Figure 3(B), $TorD^{His}$ was almost completely resistant to protease digestion, whereas the $TorA_{\Delta SP}$ was degraded to a smaller stable product. Analysis of this protease-resistant fragment by tryptic peptide mass fingerprinting showed that it was cleaved at Lys^{675}, which was the identical position where the full-length TorA precursor was cleaved. As a control, a C-terminally His-tagged, but otherwise native, form of TorA was purified from the periplasm of *E. coli* strain FTH007. The fully folded mature form of TorA was completely resistant to digestion with trypsin, even after a 16-h incubation period (Figure 3C). These results are consistent with the suggestion that the TorA–$TorD^{His}$ and $TorA_{\Delta SP}$–$TorD^{His}$ complexes have a similar overall architecture, both being susceptible to limited trypsinolysis in an identical manner. In both cases, a C-terminal stretch of immature TorA is obviously exposed to the aqueous phase in a conformation that is clearly not adopted by the mature fully assembled enzyme.

The C-terminal domain of TorA is not involved in stable TorAD complex formation

TorA is a member DMSO reductase family of molybdoenzymes. Proteins in this family adopt a fold that can be divided into four structurally distinct domains [31], and, of these, Domain IV is formed by the extreme C-terminal part of the protein and is the only domain in this fold that comprises a clear contiguous stretch of polypeptide chain (Supplementary Figure S2 at http://www.biochemj.org/bj/452/bj4520057add.htm). Although the crystal structure of the *E. coli* TorA protein has not been solved, structure predictions based on the *Shewanella massilia* TorA crystal structure [32] suggest the position of the trypsin cleavage site in the *E. coli* TorA–$TorD^{His}$ complexes lies within an unstructured loop region that connects Domain III to Domain IV (Supplementary Figure S2). To investigate this further, a construct was designed that would co-overproduce $TorD^{His}$ together with the first 675 amino acids of TorA, including the signal peptide (designated $TorA_{\Delta CT}$). First, the construct was expressed in a strain lacking endogenous TMAO reductase activity under strict anaerobic conditions, which would induce expression of the MGD biosynthetic machinery. Then a crude cell extract was prepared and the TMAO reductase activity assayed. The resultant data showed that the C-terminally truncated form of TorA was completely devoid of enzymatic activity (Supplementary Table S1 at http://www.biochemj.org/bj/452/bj4520057add.htm), establishing that this domain of the protein is absolutely critical for function. Next, $TorD^{His}$ was isolated from the soluble cell fraction by IMAC, which resulted in a protein of the expected size of $TorA_{\Delta CT}$ co-purifying (Figure 4). The two proteins remained fully associated during SEC through a Superdex 200 column (Figure 4A), with the complex eluting with an estimated molecular mass of 100 kDa (Figure 4A). Analysis of the peak fractions by SDS/PAGE confirmed that both proteins were present in the sample, but this time very little degradation of the deliberately truncated TorA was apparent (Figure 4B). SEC–MALLS analysis of the purified complex (Table 1) confirmed that the $TorA_{\Delta CT}$–$TorD^{His}$ complex had a narrow mass range of 97–107 kDa, reflecting the relative homogeneity of the sample, and a peak mass of 99.7 kDa, which is close to the calculated mass (99.2 kDa) for a 1:1 complex of the two proteins (Table 1). It can be concluded that, although the C-terminal 173 amino acids are essential for the ultimate enzymatic activity of TorA, they do not influence the formation or stability of the pre-export complex between TorA and TorD.

The TorAD complexes are devoid of MGD, but retain most of their secondary structure

Whereas it has generally been assumed that a Tat substrate protein is maintained in an 'unfolded conformation' when in complex with its pre-export chaperone, the degree of folding of such Tat precursors has not been examined in detail. In the present study, recombinant $TorD^{His}$, active $TorA^{His}$, and the TorA–$TorD^{His}$ and $TorA_{\Delta SP}$–$TorD^{His}$ complexes were analysed by CD spectroscopy. The CD spectra recorded for each sample are shown in Figure 5 and the calculated percentages of helix, strand, turn and disorder are given in Supplementary Table S2 (at http://www.biochemj.org/bj/452/bj4520057add.htm). Consistent with the highly α-helical structure of TorD [17], the CD spectrum of purified $TorD^{His}$ shows a high proportion of helix (Figure 5 and Supplementary Table S2). Enzymes of the DMSO reductase family are mixed α/β proteins [31–34] and this is reflected in the CD spectrum of purified $TorA^{His}$ (Figure 5 and Supplementary Table S2). Interestingly, CD analysis of the TorA–$TorD^{His}$ and $TorA_{\Delta SP}$–$TorD^{His}$ complexes showed that both had a significant degree of secondary structure and

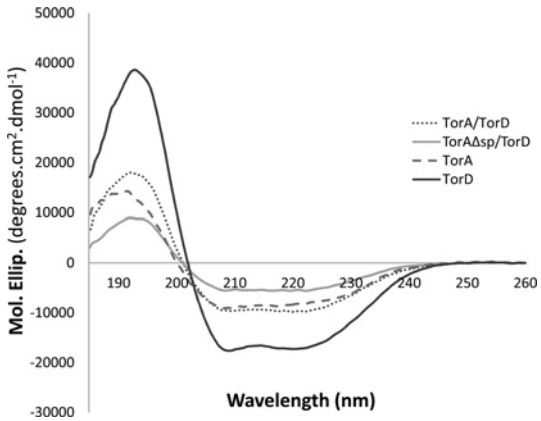

Figure 5 CD spectra of purified TorA^{His}, TorD^{His}, and the TorA–TorD^{His} and TorA$_{\Delta SP}$–TorD^{His} complexes

CD spectra (185–260 nm) were collected in quartz cells of 0.02 cm pathlength at 25 °C with a scan speed of 10 nm/min, bandwidth of 1 nm, response of 2 s and data pitch of 0.2 nm. The buffer used was 50 mM Tris/H_2SO_4 (pH 7.5), 200 mM K_2SO_4 and 1 mM DTT, and protein concentrations were: TorA, 0.7 mg/ml; TorD, 1 mg/ml; TorA–TorD^{His}, 1 mg/ml; and TorA$_{\Delta sp}$–TorD^{His}, 0.5 mg/ml.

that the observed percentage of disorder was no higher than that of isolated fully assembled TorA^{His}. Using the parameters determined for TorA^{His} and TorD^{His} (Supplementary Table S2), the predicted percentages of helix, strand, turn and disorder that would be expected for a simple 1:1 mixture of these two proteins can be calculated (Supplementary Table S2). It is notable that these predicted values are a close match to those experimentally determined for the purified TorA–TorD^{His} and TorA$_{\Delta SP}$–TorD^{His} complexes, with the values particularly close for the TorA–TorD^{His} complex (Supplementary Table S2). Taken together, these results indicate that the TorA component of the TorA–TorD^{His} complex has probably adopted its native secondary structure. Moreover, whereas the TorA^{His} protein was isolated from an anaerobic culture and exhibited a straw colour in solution, the TorA–TorD^{His} and TorA$_{\Delta SP}$–TorD^{His} complexes examined were produced from cultures grown under aerobic conditions without added molybdate. As a result, they would be expected to be largely devoid of cofactor and indeed were colourless and devoid of enzymatic activity. Metal content in the complexes by ICP-MS showed that the molar ratio of molybdenum to TorA/D complex was less than 1:1000. Taken together with the trypsinolysis experiments (Figure 3), these data suggest that the cofactor-free TorD-bound species of the TorA apoenzyme adopts a fold very similar to that of its fully assembled counterpart, save for an exposed C-terminal Domain IV.

SAXS analysis of full-length TorA–TorD^{His} and signal peptide-less TorA$_{\Delta SP}$–TorD^{His} complexes reveals shared structural features

SAXS is a powerful technique that can be used to compare the overall shapes and sizes of proteins in solution. We analysed the TorA–TorD^{His} and TorA$_{\Delta SP}$–TorD^{His} complexes, together with isolated TorD^{His}, since the high-resolution structure of TorD from *S. massilia* suggested that the protomer could adopt a highly extended conformation [17]. Representative SAXS scattering curves from each of the three samples are shown in Figure 6. It is clear that the scattering curves for the TorA–TorD^{His} and TorA$_{\Delta SP}$–TorD^{His} complexes are almost indistinguishable, indicating that they have an identical overall shape. An overview of the general parameters extracted from the SAXS data including the radii of gyration (R_g; obtained from the Guinier approximation [35]), the

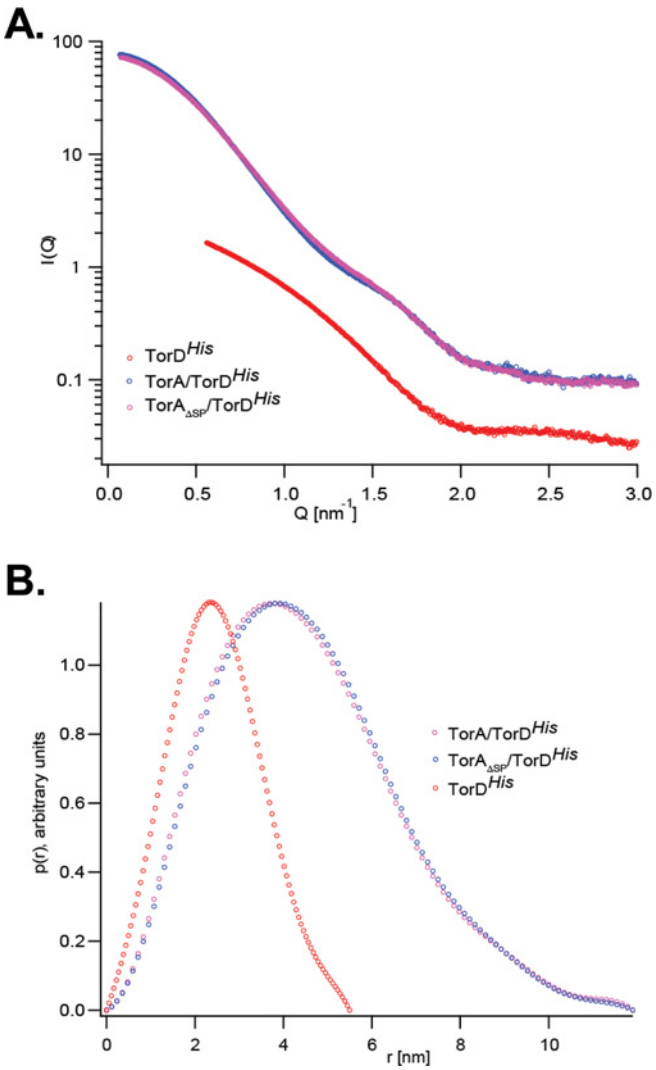

Figure 6 SAXS characterization of TorD^{His} alone and TorD^{His} in complex with different forms of TorA

(**A**) SAXS results for TorD^{His}, and the TorA–TorD^{His} and TorA$_{\Delta SP}$–TorD^{His} complexes. *Q* is the scattering vector and *I* represents intensity. (**B**) Distance distributions *P*(r) for TorD^{His}, TorA–TorD^{His} and TorA$_{\Delta SP}$–TorD^{His}. All curves were normalized.

distance distribution function, $P(r)$ and the maximum particle size (D_{max}; obtained from the GNOM [36] analysis) are given in Table 2.

A low-resolution model of TorD^{His}, obtained using the program DAMMIN [37], is shown in Figure 7(A). The overall shape of TorD^{His} is compact and elliptical with dimensions of approximately 36 Å×50 Å×34 Å. From the crystal structures of *S. massilia* TorD [17] and the TorD family protein DmsD

Table 2 SAXS parameters for the TorA and TorD proteins

This output was obtained from the scattering data and GNOM modelling for each of the indicated protein samples.

Sample	R_g (Guinier)	R_g [$P(r)$]	D_{max} [$P(r)$]
TorA–TorD^{His}	35.0 Å	35.2 Å	119 Å
TorA$_{\Delta SP}$–TorD^{His}	35.6 Å	35.1 Å	119 Å
TorD^{His}	20.0 Å	19.2 Å	55 Å

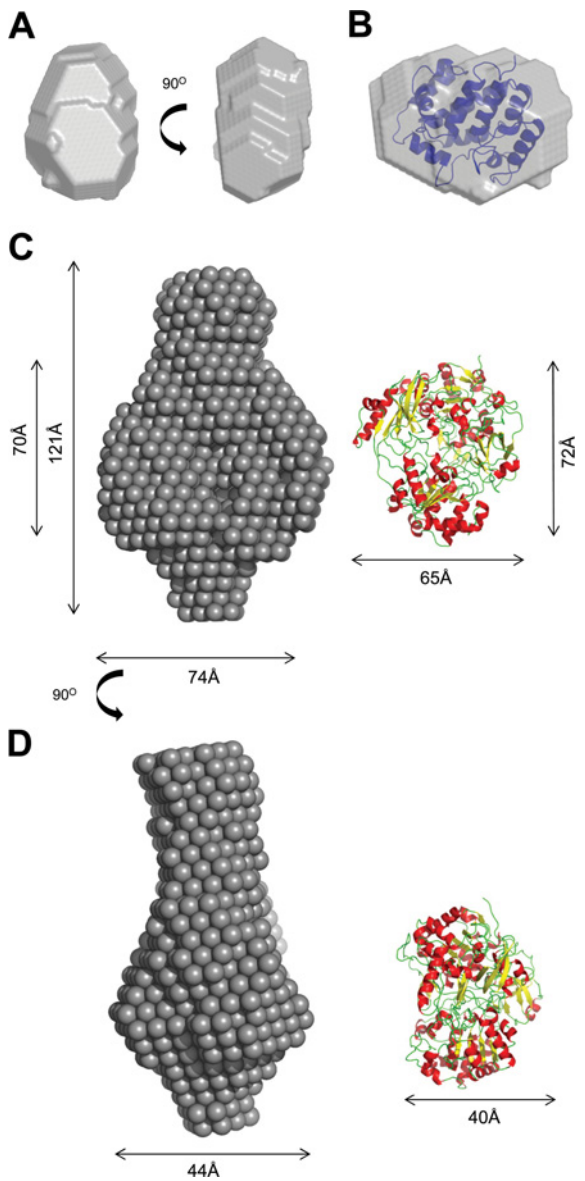

Figure 7 ***Ab initio*** **modelling of TorD^{His} and the TorA–TorD^{His} complex**

(**A**) Two different views of the *ab intio* model of TorD, generated using DAMMIN [37]. (**B**) The electron density for *E. coli* DmsD (PDB code 3CW0 [39]) docked into the SAXS-derived shape of TorD^{His}. (**C**) and (**D**) represent two different views of the *ab intio* model of the TorA–TorD^{His} complex. The X-ray structure of *S. massilia* TorA (PDB code 1TMO [32]) is shown to the right.

from *E. coli* [38–40], scattering envelopes can be calculated [41]. It is clear from Supplementary Figure S3 (http://www.biochemj.org/bj/452/bj4520057add.htm) that neither the *S. massilia* TorD domain-swapped dimer nor one of the protomers involved in forming that dimer would give scattering curves similar to that measured for TorD^{His} in solution. By contrast, the scattering curve predicted from the X-ray structure of DmsD is very similar in shape, and the electron density of monomeric DmsD, which can be readily docked into the TorD^{His} SAXS envelope (Figure 7B).

Since the scattering curves indicated that the TorA–TorD^{His} and TorA$_{\Delta SP}$–TorD^{His} complexes were indistinguishable, a single SAXS-derived shape corresponding to either the TorA–TorD^{His} or the TorA$_{\Delta SP}$–TorD^{His} complex is shown in Figures 7(C) and 7(D). The complex is highly elongated, with an overall length of approximately 120 Å. There is a large central area of density with one relatively large lobe of density protruding from one side of the central region and a smaller lobe of density protruding from the opposite side. The large central area has approximate dimensions of 70 Å×74 Å×44 Å and is a reasonably close match to the dimensions of the crystal structure of *S. massilia* TorA (Figures 7C and 7D).

DISCUSSION

The process of co-ordinated assembly ('proofreading' or 'quality control') is an important consideration in the biosynthesis of all complex cofactor-containing Tat-dependent enzymes [5]. The simplest model system used to study this process is the *E. coli* TMAO reductase, which has a single MGD cofactor and a single biosynthetic chaperone, TorD. Whereas early research has seen analyses of the TorD–signal peptide interaction in isolation [12,42], the present study has focused on the characterization of the entire pre-export TorAD complex.

Design of co-overproduction vectors established that untagged TorA formed a tight and stable complex with hexahistidine-tagged TorD. Surprisingly, however, despite the strong evidence for two separate TorD-binding sites on TorA [9,11], we have clearly demonstrated using the accurate SEC–MALLS technique in conjunction with other experiments that TorD binds TorA with a 1:1 stoichiometry. Even more surprisingly, given the well-characterized interaction between TorD and the TorA signal peptide [11–15,42], a truncated TorA enzyme completely lacking its entire 39-residue signal peptide retained the ability to interact in a stable manner with TorD. Whereas the present study clearly establishes that there is a high-affinity TorD-binding site within the mature portion of TorA, it also raises questions about the role and importance of the signal peptide interaction.

These findings can be interpreted in two possible ways. First, that the signal peptide-binding activity of TorD is of a much lower affinity than that of the second binding site within the mature TorA sequence, so much so that there is a strong bias towards the higher-affinity species during the purification protocol. Although this scenario is not impossible, recent studies place the apparent K_d for TorD binding to the isolated TorA signal peptide at 59–330 nM [12,42], which is indicative of very tight binding such that it is likely that a detectable portion of TorA would not fail to have two TorD molecules bound. The second possibility is that the TorD-binding site within the mature portion of TorA is very close to the signal peptide-binding epitope such that a single TorD protein could interact with both simultaneously. This hypothesis would require there to be two different TorA-binding sites on a single TorD protein. Although the location of the TorA signal peptide-binding site on TorD has not yet been reported, there is a larger body of evidence available on the location of the signal peptide-binding site on another member of the TorD family, DmsD. The *E. coli* DmsD protein was the first twin-arginine signal peptide-binding chaperone to be described [43]. It is essential for the assembly of molybdenum-dependent DMSO reductase and selenate reductase enzymes in *E. coli* and binds to the signal peptides of those enzymes with apparent K_d values in the range 10–100 nM [43–45]. Genetic, biochemical and structural analyses predict the signal peptide-binding site to occupy only one face of DmsD (primarily involving residues of the N-terminal helices) and so suggests that a significant proportion the DmsD protein is not involved in signal peptide recognition [39,45,46]. This leaves the possibility, at least, that a second protein- or peptide-recognition site may be present on this type of chaperone. Indeed, variants of *E. coli* TorD have been described (C79R and L83P)

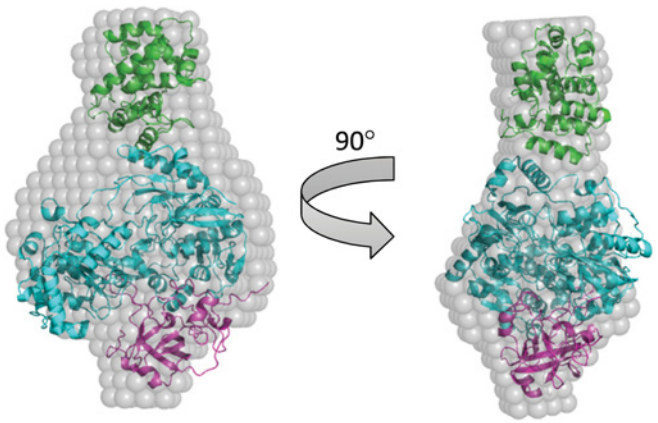

Figure 8 Rigid body modelling of the TorA–TorD^{His} complex

Rigid body modelling was conducted using the homologous component parts of the complex, i.e. TorD homologue DmsD (PDB code 3CW0, shown in green), and TorA (PDB code 1TMO) split into two parts: Domains I–III (i.e. amino acids 5–629; shown in cyan) and Domain IV (amino acids 631–798; shown in magenta). Modelling was conducted using SASREF [47]. The generated model is docked into the TorA–TorD^{His} *ab intio* model for comparison.

that retain signal peptide-binding activity, but are impaired in their binding to mature TorA [10].

Further evidence for overlapping TorD-binding sites near the N-terminus of TorA come from analysis of the SAXS data obtained in the present study. To investigate the possible arrangement of TorA and TorD in the TorAD complex, rigid body modelling was undertaken using the SASREF program [47] and the structures of *S. massilia* TorA and *E. coli* DmsD as building blocks. To facilitate this analysis, TorA was split into two parts to give the proteolytically stable N-terminal part (Domains I–III) and the proteolytically sensitive Domain IV identified in the present study. A constraint was then applied that the last amino acid of N-terminal part should be within 10 Å of the first amino acid of Domain IV, in order to incorporate flexibility into the TorA component of the complex, again consistent with the protease accessibility results of the present study. The results from the rigid body modelling show a similar overall shape to that obtained during *ab initio* analysis (the fit of the model with the experimental data is shown in Supplementary Figure S4 at http://www.biochemj.org/bj/452/bj4520057add.htm). The rigid body model is shown docked into the *ab initio* SAXS-derived envelope of TorAD in Figure 8. When docked into the *ab initio* model, the density for TorD fits very well into the larger protruding lobe, whereas the remainder of the *ab initio* envelope is of an appropriate volume to accommodate TorA. The C-terminal Domain IV of TorA distal from TorD fits into the smaller protruding lobe, which is consistent with the biochemical data of the present study that Domain IV is not required for interaction of TorD with TorA. Bearing in mind that the SAXS scattering curves for both signal peptide-containing and signal peptide-free TorAD complexes are identical, this must be taken as good evidence that the binding epitope for TorD on the mature portion of TorA must lie near the N-terminus and thus also near the second epitope within the signal peptide.

The CD and SAXS analyses suggest that there is a very high degree of folding by the TorA protein even in the absence of the MGD cofactor. However, it is clear that the TorA–TorD^{His} and TorA$_{\Delta SP}$–TorD^{His} complexes are not in the native conformation and that the C-terminal Domain IV of the TorA protein is exposed. This could suggest that the locking of Domain IV into position represents the final act in cofactor insertion. One possible role of TorD could be to prevent premature closing of the Domain IV 'flap' before MGD has bound, or, alternatively, that closing of Domain IV after cofactor loading is the trigger that releases TorD from the now mature enzyme. The molecular mechanism of how TorD senses the events surrounding cofactor loading remains to be unearthed.

AUTHOR CONTRIBUTION

Jennifer Dow, Frank Gabel, Frank Sargent and Tracy Palmer performed the research and analysed data; Jennifer Dow, Frank Sargent and Tracy Palmer designed the research; Tracy Palmer supervised the research; and Jennifer Dow, Frank Gabel, Frank Sargent and Tracy Palmer wrote the paper.

ACKNOWLEDGEMENTS

We acknowledge Dr Bérengère Ize, Dr Grant Buchanan and Dr Dave Guymer for useful discussions and preliminary studies. We also thank Dr Cyril Dian for technical assistance at the ID14-3 BioSAXS beamline at the ESRF.

FUNDING

This work was funded via a Wellcome Trust Ph.D. Studentship Award to J.M.D. [grant number WT089692/Z09/z] and a Royal Society Wolfson Research Merit Award to T.P.

REFERENCES

1 Celedon, J. M. and Cline, K. (2013) Intra-plastid protein trafficking: how plant cells adapted prokaryotic mechanisms to the eukaryotic condition. Biochim. Biophys. Acta **1833**, 341–351
2 Palmer, T. and Berks, B. C. (2012) The twin-arginine translocation (Tat) protein export pathway. Nat. Rev. Microbiol. **10**, 483–496
3 Berks, B. C. (1996) A common export pathway for proteins binding complex redox cofactors? Mol. Microbiol. **22**, 393–404
4 Palmer, T., Sargent, F. and Berks, B. C. (2010) The Tat protein export pathway. In EcoSal–*Escherichia coli* and *Salmonella*: Cellular and Molecular Biology, Chapter 4.3.2, http://www.ecosal.org (Böck, A., Curtiss, R., Kaper, J. B., Karp, P. D., Neidhardt, F. C., Nyström, T., Slauch, J. M., Squires, C. L. and Ussery, D., eds), ASM Press, Washington, DC
5 Sargent, F. (2007) Constructing the wonders of the bacterial world: biosynthesis of complex enzymes. Microbiology **153**, 633–651
6 Silvestro, A., Pommier, J. and Giordano, G. (1988) The inducible trimethylamine-*N*-oxide reductase of *Escherichia coli* K12: biochemical and immunological studies. Biochim. Biophys. Acta **954**, 1–13
7 Santini, C. L., Ize, B., Chanal, A., Müller, M., Giordano, G. and Wu, L. F. (1998) A novel sec-independent periplasmic protein translocation pathway in *Escherichia coli*. EMBO J. **17**, 101–112
8 Mejean, V., Iobbi-Nivol, C., Lepelletier, M., Giordano, G., Chippaux, M. and Pascal, M. C. (1994) TMAO anaerobic respiration in *Escherichia coli*: involvement of the *tor* operon. Mol. Microbiol. **11**, 1169–1179
9 Pommier, J., Mejean, V., Giordano, G. and Iobbi-Nivol, C. (1998) TorD, a cytoplasmic chaperone that interacts with the unfolded trimethylamine *N*-oxide reductase enzyme (TorA) in *Escherichia coli*. J. Biol. Chem. **273**, 16615–16620
10 Genest, O., Neumann, M., Seduk, F., Stocklein, W., Mejean, V., Leimkuhler, S. and Iobbi-Nivol, C. (2008) Dedicated metallochaperone connects apoenzyme and molybdenum cofactor biosynthesis components. J. Biol. Chem. **283**, 21433–21440
11 Jack, R. L., Buchanan, G., Dubini, A., Hatzixanthis, K., Palmer, T. and Sargent, F. (2004) Coordinating assembly and export of complex bacterial proteins. EMBO J. **23**, 3962–3972
12 Buchanan, G., Maillard, J., Nabuurs, S. B., Richardson, D. J., Palmer, T. and Sargent, F. (2008) Features of a twin-arginine signal peptide required for recognition by a Tat proofreading chaperone. FEBS Lett. **582**, 3979–3984
13 Hatzixanthis, K., Clarke, T. A., Oubrie, A., Richardson, D. J., Turner, R. J. and Sargent, F. (2005) Signal peptide–chaperone interactions on the twin-arginine protein transport pathway. Proc. Natl. Acad. Sci. U.S.A. **102**, 8460–8465
14 Genest, O., Seduk, F., Ilbert, M., Mejean, V. and Iobbi-Nivol, C. (2006) Signal peptide protection by specific chaperone. Biochem. Biophys. Res. Commun. **339**, 991–995

15 Li, S. Y., Chang, B. Y. and Lin, S. C. (2006) Coexpression of TorD enhances the transport of GFP via the TAT pathway. J. Biotechnol. **122**, 412–421
16 Tranier, S., Mortier-Barriere, I., Ilbert, M., Birck, C., Iobbi-Nivol, C., Mejean, V. and Samama, J. P. (2002) Characterization and multiple molecular forms of TorD from *Shewanella massilia*, the putative chaperone of the molybdoenzyme TorA. Protein Sci. **11**, 2148–2157
17 Tranier, S., Iobbi-Nivol, C., Birck, C., Ilbert, M., Mortier-Barriere, I., Mejean, V. and Samama, J. P. (2003) A novel protein fold and extreme domain swapping in the dimeric TorD chaperone from *Shewanella massilia*. Structure **11**, 165–174
18 Guymer, D., Maillard, J., Agacan, M. F., Brearley, C. A. and Sargent, F. (2010) Intrinsic GTPase activity of a bacterial twin-arginine translocation proofreading chaperone induced by domain swapping. FEBS J. **277**, 511–525
19 Genest, O., Neumann, M., Seduk, F., Stocklein, W., Mejean, V., Leimkuhler, S. and Iobbi-Nivol, C. (2008) Dedicated metallochaperone connects apoenzyme and molybdenum cofactor biosynthesis components. J. Biol. Chem. **283**, 21433–21440
20 Genest, O., Mejean, V. and Iobbi-Nivol, C. (2009) Multiple roles of TorD-like chaperones in the biogenesis of molybdoenzymes. FEMS Microbiol. Lett. **297**, 1–9
21 Butland, G., Peregrin-Alvarez, J. M., Li, J., Yang, W., Yang, X., Canadien, V., Starostine, A., Richards, D., Beattie, B., Krogan, N. et al. (2005) Interaction network containing conserved and essential protein complexes in *Escherichia coli*. Nature **433**, 531–537
22 Ize, B., Coulthurst, S. J., Hatzixanthis, K., Caldelari, I., Buchanan, G., Barclay, E. C., Richardson, D. J., Palmer, T. and Sargent, F. (2009) Remnant signal peptides on non-exported enzymes: implications for the evolution of prokaryotic respiratory chains. Microbiology **155**, 3992–4004
23 de Leeuw, E., Granjon, T., Porcelli, I., Alami, M., Carr, S. B., Müller, M., Sargent, F., Palmer, T. and Berks, B. C. (2002) Oligomeric properties and signal peptide binding by *Escherichia coli* Tat protein transport complexes. J. Mol. Biol. **322**, 1135–1146
24 Hamilton, C. M., Aldea, M., Washburn, B. K., Babitzke, P. and Kushner, S. R. (1989) New method for generating deletions and gene replacements in *Escherichia coli*. J. Bacteriol. **171**, 4617–4622
25 Sambasivarao, D. and Weiner, J. H. (1991) Dimethyl sulfoxide reductase of *Escherichia coli*: an investigation of function and assembly by use of *in vivo* complementation. J. Bacteriol. **173**, 5935–5943
26 Sargent, F., Bogsch, E. G., Stanley, N. R., Wexler, M., Robinson, C., Berks, B. C. and Palmer, T. (1998) Overlapping functions of components of a bacterial Sec-independent protein export pathway. EMBO J. **17**, 3640–3650
27 Palmer, T., Berks, B. C. and Sargent, F. (2010) Analysis of Tat targeting function and twin-arginine signal peptide activity in *Escherichia coli*. Methods Mol. Biol. **619**, 191–216
28 Lowry, O. H., Rosebrough, N. J., Farr, A. L. and Randall, R. J. (1951) Protein measurement with the Folin phenol reagent. J. Biol. Chem. **193**, 265–275
29 Konarev, P. V., Volkov, V. V., Sokolova, A. V., Koch, M. H. J. and Svergun, D. I. (2003) PRIMUS: a Windows-PC based system for small-angle scattering data analysis. J. Appl. Crystallogr. **36**, 1277–1282
30 Zimm, B. H. (1948) The scattering of light and the radial distribution function of high polymer solutions. J. Chem. Phys. **16**, 1093–1099
31 Schindelin, H., Kisker, C., Hilton, J., Rajagopalan, K. V. and Rees, D. C. (1996) Crystal structure of DMSO reductase: redox-linked changes in molybdopterin coordination. Science **272**, 1615–1621
32 Czjzek, M., Dos Santos, J. P., Pommier, J., Giordano, G., Mejean, V. and Haser, R. (1998) Crystal structure of oxidized trimethylamine *N*-oxide reductase from *Shewanella massilia* at 2.5 Å resolution. J. Mol. Biol. **284**, 435–447
33 Schneider, F., Lowe, J., Huber, R., Schindelin, H., Kisker, C. and Knablein, J. (1996) Crystal structure of dimethyl sulfoxide reductase from *Rhodobacter capsulatus* at 1.88 Å resolution. J. Mol. Biol. **263**, 53–69
34 McAlpine, A. S., McEwan, A. G. and Bailey, S. (1998) The high resolution crystal structure of DMSO reductase in complex with DMSO. J. Mol. Biol. **275**, 613–623
35 Guinier, A. (1939) La diffraction des rayons X aux tres faibles angles: applications a l'etude des phenomenes ultra-microscopiques. Ann. Phys. **12**, 161–236
36 Svergun, D. I. (1992) Determination of the regularization parameter in indirect-transform methods using perceptual criteria. J. Appl. Crystallogr. **25**, 495–503
37 Svergun, D. I. (1999) Restoring low resolution structure of biological macromolecules from solution scattering using simulated annealing. Biophys. J. **76**, 2879–2886
38 Stevens, C. M., Winstone, T. M., Turner, R. J. and Paetzel, M. (2009) Structural analysis of a monomeric form of the twin-arginine leader peptide binding chaperone *Escherichia coli* DmsD. J. Mol. Biol. **389**, 124–133
39 Ramasamy, S. K. and Clemons, Jr, W. M. (2009) Structure of the twin-arginine signal-binding protein DmsD from *Escherichia coli*. Acta Crystallogr., Sect. F: Struct. Biol. Crystal. Commun. **65**, 746–750
40 Qiu, Y., Zhang, R., Binkowski, T. A., Tereshko, V., Joachimiak, A. and Kossiakoff, A. (2008) The 1.38 Å crystal structure of DmsD protein from *Salmonella typhimurium*, a proofreading chaperone on the Tat pathway. Proteins **71**, 525–533
41 Svergun, D., Barberato, C. and Koch, M. H. J. (1995) CRYSOL: a program to evaluate x-ray solution scattering of biological macromolecules from atomic coordinates. J. Appl. Crystallogr. **28**, 768–773
42 Shanmugham, A., Bakayan, A., Voller, P., Grosveld, J., Lill, H. and Bollen, Y. J. (2012) The hydrophobic core of twin-arginine signal sequences orchestrates specific binding to Tat-pathway related chaperones. PLoS ONE **7**, e34159
43 Oresnik, I. J., Ladner, C. L. and Turner, R. J. (2001) Identification of a twin-arginine leader-binding protein. Mol. Microbiol. **40**, 323–331
44 Guymer, D., Maillard, J. and Sargent, F. (2009) A genetic analysis of *in vivo* selenate reduction by *Salmonella enterica* serovar Typhimurium LT2 and *Escherichia coli* K12. Arch. Microbiol. **191**, 519–528
45 Chan, C. S., Winstone, T. M., Chang, L., Stevens, C. M., Workentine, M. L., Li, H., Wei, Y., Ondrechen, M. J., Paetzel, M. and Turner, R. J. (2008) Identification of residues in DmsD for twin-arginine leader peptide binding, defined through random and bioinformatics-directed mutagenesis. Biochemistry **47**, 2749–2759
46 Stevens, C. M., Okon, M., McIntosh, L. P. and Paetzel, M. (2012) ^{1}H, ^{13}C and ^{15}N resonance assignments and peptide binding site chemical shift perturbation mapping for the *Escherichia coli* redox enzyme chaperone DmsD. Biomol. NMR Assign., doi:10.1007/s12104-012-9408-8
47 Petoukhov, M. V. and Svergun, D. I. (2005) Global rigid body modeling of macromolecular complexes against small-angle scattering data. Biophys. J. **89**, 1237–1250

Received 7 December 2012/5 February 2013; accepted 1 March 2013
Published as BJ Immediate Publication 1 March 2013, doi:10.1042/BJ20121832

Biochem. J. (2013) **452**, 57–66 (Printed in Great Britain) doi:10.1042/BJ20121832

SUPPLEMENTARY ONLINE DATA

Characterization of a pre-export enzyme–chaperone complex on the twin-arginine transport pathway

Jennifer M. DOW*, Frank GABEL†, Frank SARGENT*[1] and Tracy PALMER*[1]

*Division of Molecular Microbiology, College of Life Sciences, University of Dundee, Dundee DD1 5EH, U.K., and †Institut de Biologie Structurale, Commissariat à l'Energie Atomique, CNRS, Université Joseph Fourier, 41 rue Jules Horowitz, 38027 Grenoble, France

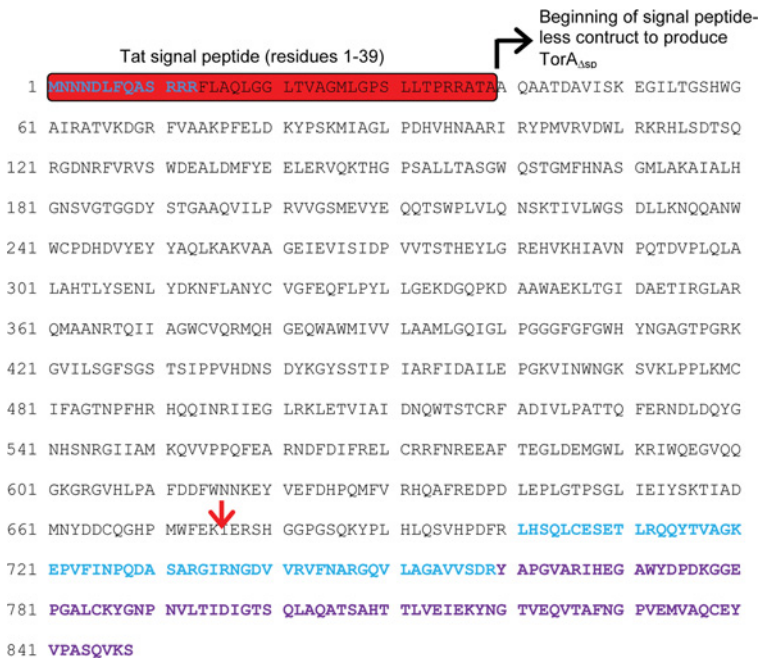

Figure S1 The *E. coli* TorA precursor primary sequence

The points of natural proteolysis, and deliberate truncation, of the TorA precursor are highlighted. The 39-residue N-terminal twin-arginine signal peptide is highlighted in red. The position of the engineered initiation site for the construct expressing the signal-less TorA protein is indicated by the black arrow. The location of the experimentally determined trypsin-cleavage site for TorA within the TorA–TorD^{His} complex is indicated by the red arrow. This is also the point of truncation for the TorA$_{\Delta CT}$ protein. A small fraction of the TorA sample is subject to degradation during the purification procedure. Following IMAC, a small fraction of TorA is found to be degraded from the C-terminus and loses the purple-coloured stretch of polypeptide. Following the subsequent SEC step, a small fraction of TorA within the TorA–TorD^{His} complex becomes proteolysed at the N-terminus and further at the C-terminus (blue). This shows that the extremities of TorA are not shielded or protected by the tightly bound TorD^{His} protein, are exposed to solvent and are therefore susceptible to proteolysis.

[1] Correspondence may be addressed to either of these authors (email f.sargent@dundee.ac.uk or t.palmer@dundee.ac.uk).

Figure S2 X-ray structure of *S. massilia* TorA

The C-terminal Domain IV is shaded in blue and the approximate position of the trypsin-cleavage site determined for *E. coli* TorA in the TorA–TorD^{His} and TorA$_{\Delta SP}$–TorD^{His} complexes is indicated. The image was created using PyMOL (http://www.pymol.org) with PDB code 1TMO.

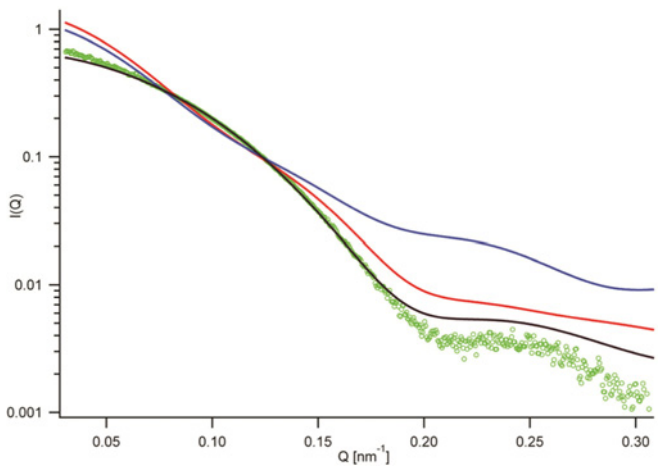

Figure S3 Comparison of SAXS scattering curves

Theoretical curves were calculated from *S. massilia* TorD (PDB code 1N1C) monomer (blue line) and dimer (red line) and *E. coli* DmsD (PDB code 3CW0) monomer (black line) using CRYSOL and compared with experimental scattering curves of TorD^{His} (green dots).

Received 7 December 2012/5 February 2013; accepted 1 March 2013
Published as BJ Immediate Publication 1 March 2013, doi:10.1042/BJ20121832

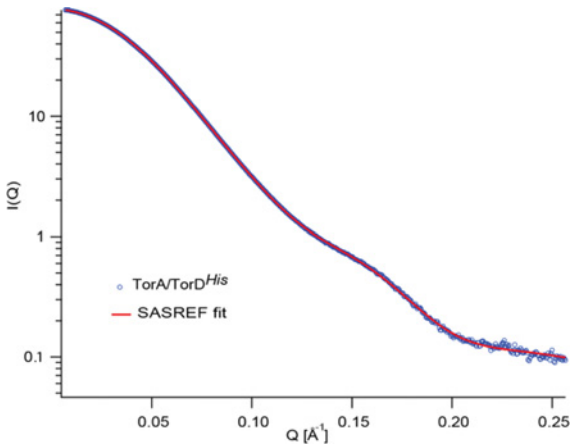

Figure S4 SAXS scattering curve of the TorA–TorD^{His} complex

Fitted curve of TorAD^{His} rigid body modelling conducted using the TorA structure (PDB code 1TMO) (split into two components: Domains I–III and Domain IV) and the DmsD structure (PDB code 3CW0), performed using SASREF. The fitted curve is shown in comparison with the *E. coli* TorAD^{His} scattering curve.

Table S1 TMAO reductase activity in strains producing variants of TorA

Crude cell extracts were prepared from anaerobically grown cells before TMAO-dependent Benzyl Viologen-oxidation assays were performed. Results are means ± S.D. of three measurements.

Strain and plasmid	Complex produced	TMAO reductase activity (μmol of Benzyl Viologen oxidized/min per mg of protein)
GB426 (*tor*$^-$, *dms*$^-$) + pQE80 (control)	–	0.15 ± 0.01
GB426 + pQE80TorADHis	TorA/TorD^{His}	28.8 ± 4.0
GB426 + pQE80TorAdelSSDHis	TorA$_{\Delta SP}$/TorD^{His}	14.8 ± 1.6
GB426 + pQE80TorAtruncDhis	TorA$_{\Delta CT}$/TorD^{His}	0.12 ± 0.01

Table S2 Characterization of the TorA and TorD proteins by CD

Proportions of secondary-structural elements were calculated from CD analysis for each of the indicated samples.

Protein	Total helix (%)	Total strand (%)	Turns (%)	Unordered (%)
TorA^{His} (experimental)	26	25	20	29
TorD^{His} (experimental)	56	7	17	20
TorA^{His} and TorD^{His} combined (theoretical)	31	22	19	27
TorA–TorD^{His} (experimental)	28	22	22	29
TorA$_{\Delta SP}$–TorD^{His} (experimental)	20	29	22	30